catalysts

MDPI

Article

Ultrasound/Chlorine: A Novel Synergistic Sono-Hybrid Process for Allura Red AC Degradation

Oualid Hamdaoui [1,*], Slimane Merouani [2], Hadjer C. Benmahmoud [3], Meriem Ait Idir [3], Hamza Ferkous [3] and Abdulaziz Alghyamah [1]

[1] Chemical Engineering Department, College of Engineering, King Saud University, P.O. Box 800, 11421 Riyadh, Saudi Arabia
[2] Laboratory of Environmental Process Engineering, Department of Chemical Engineering, Faculty of Process Engineering, University Salah Boubnider Constantine 3, P.O. Box 72, Constantine 25000, Algeria
[3] Process Engineering Department, Faculty of Technology, Badji Mokhtar Annaba University, P.O. Box 12, Annaba 23000, Algeria
* Correspondence: ohamdaoui@ksu.edu.sa or ohamdaoui@yahoo.fr

Abstract: Herein, we present an original report on chlorine activation by ultrasound (US: 600 kHz, 120 W) for intensifying the sonochemical treatment of hazardous organic materials. The coupling of US/chlorine produced synergy via the involvement of reactive chlorine species (RCSs: $Cl^{\bullet}$, $ClO^{\bullet}$ and $Cl_2^{\bullet-}$), resulting from the sono-activation of chlorine. The degradation of Allura Red AC (ARAC) textile dye, as a contaminant model, was drastically improved by the US/chlorine process as compared to the separated techniques. A synergy index of 1.74 was obtained by the US/chlorine process for the degradation of ARAC (C_0 = 5 mg·L^{-1}) at pH 5.5 and [chlorine]$_0$ = 250 mM. The synergistic index increased by up to 2.2 when chlorine concentration was 300 µM. Additionally, the synergetic effect was only obtained at pH 4–6, where HOCl is the sole chlorine species. Additionally, the effect of combining US and chlorine for ARAC degradation was additive for the argon atmosphere, synergistic for air and negative for N_2. An air atmosphere could provide the best synergy as it generates a relatively moderate concentration of reactive species as compared to argon, which marginalizes radical–radical reactions compared to radical–organic ones. Finally, the US/chlorine process was more synergistic for low pollutant concentrations ($C_0 \leq 10$ mg·L^{-1}); the coupling effect was additive for moderate concentrations (C_0~20–30 mg·L^{-1}) and negative for higher C_0 (>30 mg·L^{-1}). Consequently, the US/chlorine process was efficiently operable under typical water treatment conditions, although complete by-product analysis and toxicity assessment may still be necessary to establish process viability.

Keywords: ultrasound/chlorine process; reactive chlorine species (RCS); Allura Red AC (ARAC); degradation; synergy

check for updates

Citation: Hamdaoui, O.; Merouani, S.; Benmahmoud, H.C.; Ait Idir, M.; Ferkous, H.; Alghyamah, A. Ultrasound/Chlorine: A Novel Synergistic Sono-Hybrid Process for Allura Red AC Degradation. *Catalysts* **2022**, *12*, 1171. https: doi.org/10.3390/catal12101171

Academic Editors: Gassan Hodaifa, Rafael Borja and Mha Albqmi

Received: 9 September 2022
Accepted: 30 September 2022
Published: 4 October 2022

Publisher's Note: MDPI stays neutral with regard to jurisdictional claims in published maps and institutional affiliations.

Copyright: © 2022 by the authors. Licensee MDPI, Basel, Switzerland. This article is an open access article distributed under the terms and conditions of the Creative Commons Attribution (CC BY) license (https://creativecommons.org/licenses/by/4.0/).

1. Introduction

Due to the high chemical stability and/or low biodegradability of most of water contaminants, one feasible option for removing organic pollutants from wastewater is the use of advanced oxidation processes (AOPs) [1]. These processes, e.g., Fe(II)/H_2O_2 (or $S_2O_8^{2-}$), UV/H_2O_2 (or $S_2O_8^{2-}$), UV/O_3, H_2O_2/O_3 and UV/TiO_2, have been widely recognized as highly effective treatments for recalcitrant wastewater or as a pretreatment to convert micropollutants into shorter chain substrates that can then be treated using conventional biological methods [2]. AOPs generate reactive free radicals, i.e., $^{\bullet}OH$ (E^0 = 2.8 V/NHE) or ($SO_4^{\bullet-}$, E^0 = 2.6 V/NHE), that are non-selective and highly reactive toward most organic pollutants [3,4].

High-power ultrasound (US: 100–1000 kHz) is one tool to generate $^{\bullet}OH$ radicals for water treatment applications [5]. Water sonolysis creates cavitation bubbles, which grow

and collapse implosively in a time scale of microseconds, generating extreme temperatures and pressures within the bubbles (~5000 K and ~1000 atm) [6]. Radicals such as $^{\bullet}OH$, $H^{\bullet}$ and $HO_2^{\bullet}$, and atomic oxygen (O) are formed as a consequence of the pyrolytic reactions inside the bubble, under the extraordinary temperature developed at the final stage of the collapse [7–9]. The formation mechanism of these reactive moieties begins with the homolytic cleavage of water vapor and O_2 trapped inside the bubble to form $^{\bullet}OH$, $H^{\bullet}$ and O atoms (i.e., $H_2O \rightarrow {}^{\bullet}OH + H^{\bullet}$ and $O_2 \rightarrow 2O$) [10,11]. These primary species can react with H_2O or O_2 molecules to produce other reactive species such as $HO_2^{\bullet}$ (i.e., $H^{\bullet} + O_2 \rightarrow HO_2^{\bullet}$). Upon collapse, these radicals can diffuse into the bubble/solution interface to recombine or react with solutes present at the interfacial region. H_2O_2 is the main product of radicals' recombination at the bubble/solution interface, i.e., $2{}^{\bullet}OH \rightarrow H_2O_2$ and $2HO_2^{\bullet} \rightarrow H_2O_2 + O_2$. Some radical reactions can also take place in the liquid bulk as ~10% of the formed radicals can reach the solution zone [12]. The hydroxyl radical is the most important radical implicated in the sonochemical treatment of hydrophobic/hydrophilic organic pollutants [5]. Parallel reaction pathways exist whereby volatile solutes may evaporate into the bubble and be pyrolyzed by the high core temperatures [13].

Recently, UV light and iron have been reported as efficient activators of chlorine for AOP-applications [14–16]. The UV/chlorine and Fe(II)/chlorine systems are emerging as attractive alternatives to UV/H_2O_2 and Fe(II)/H_2O_2 traditional AOPs. The interaction between UV light (<400 nm) or iron with chlorine can produce $^{\bullet}OH$ and $Cl^{\bullet}$ as initial reactive species (Equations (1)–(4)) [16,17]. These radicals can then drive a reaction chain in which additional reactive chlorine species (RCSs), such as $ClO^{\bullet}$ and $Cl_2^{\bullet-}$, can be formed. $ClO^{\bullet}$ forms via a reaction of $Cl^{\bullet}$ or $^{\bullet}OH$ with chlorine, while $Cl_2^{\bullet-}$ forms via a reaction of $Cl^{\bullet}$ with Cl^-. Interesting work on oxidant formation mechanisms in UV/chlorine and Fe(II)/chlorine systems and their subsequent reactions with organics has been delivered by many researchers [14–20].

$$HClO + h\nu \rightarrow {}^{\bullet}OH + Cl^{\bullet} \quad k_1 = \sim 1.3\times10^{-3}\ s^{-1} \tag{1}$$

$$ClO^- + h\nu \rightarrow O^{\bullet-} + Cl^{\bullet} \quad k_2 = 9\times10^{-3}\ s^{-1} \tag{2}$$

$$Fe(II) + HClO \rightarrow Fe(III) + {}^{\cdot}OH + Cl^- \quad k_3 = \sim 10^4\ M^{-1}\ s^{-1} \tag{3}$$

$$Fe(II) + HClO \rightarrow Fe(III) + Cl^{\cdot} + OH^- \quad k_4 = \sim 10^4\ M^{-1}\ s^{-1} \tag{4}$$

The generated reactive chlorine species (RCSs: $Cl^{\bullet}$, $ClO^{\bullet}$ and $Cl_2^{\bullet-}$) are of high redox potentials (2.43 V/NHE for $Cl^{\bullet}$, 2.13 V/NHE for $Cl_2^{\bullet-}$ and 1.5–1.8 V/NHE for $ClO^{\bullet}$) and are mostly implicated in the destruction of several water contaminants [21–32]. Unlike $^{\bullet}OH$, RCSs are selective oxidants that preferentially react with electron-rich moieties [33]. These radicals react with organic matter practically with the same mechanisms as those of $^{\bullet}OH$ (i.e., H-atom abstraction, electron transfer or addition to unsaturated bands) [14]. The second-order rate constants for reactions involving RCS radicals varies in the order of ~10^8–10^{11} $M^{-1}\cdot s^{-1}$ for $Cl^{\bullet}$, ~10^7–10^9 $M^{-1}\cdot s^{-1}$ for $ClO^{\bullet}$ and 10^2–10^6 $M^{-1}\cdot s^{-1}$ for $Cl_2^{\bullet-}$ [14,15]. Additionally, RCSs have been characterized by a longer lifetime than that of $^{\bullet}OH$, i.e., 5 μs for $Cl^{\bullet}$ [34] and fractions of milliseconds for $Cl_2^{\bullet-}$ [34], making them available for longer in the solution. All these advantageous specifications of RCSs make them efficient oxidation agents that may create a parallel degradation pathway to that of $^{\bullet}OH$, thereby accelerating the degradation of micropollutants. Due to the significant implication of RCSs in the UV/chlorine system, this process was found to be more efficient in degrading several water contaminants than UV/H_2O_2 [25].

Chlorine is globally the most used chemical oxidant for drinking water disinfection and it led to the formation of trihalomethanes and haloacetic acids. Despite its low activity on microorganisms in biofilms, chlorine can lead to a significant removal of the majority of planktonic bacteria [35]. The combination of ultrasound with chlorine can improve the disinfection process, with the advantage of preventing the formation of disinfection by-products and reducing the chlorine dosage required for achieving admissible disinfec-

tion efficiencies [36]. Despite numerous reports of using acoustic cavitation to accelerate wastewater disinfection processes [36–38], the application of the US/chlorine system as an oxidation technique for the degradation of organic pollutants is, unexpectedly, very scarce [39]. The US/chlorine technique may present numerous preliminary advantages [39]:

- Chlorine is easy to handle, with more safety, as it is less harmful than other oxidants. Furthermore, the liquid phase of chlorine simplifies its use.
- Chlorine is more available and less expensive than other oxidants that require in situ production via a sophisticated expensive device. Consequently, the cost of the US/chlorine technique could be lower than other processes for similar experimental conditions.
- The US/chlorine treatment does not necessitate elimination of the residual chlorine as it is originally employed as a disinfectant.

In this work, chlorine activation by US as a new promising sono-hybrid advanced oxidation process is investigated, using Allura Red AC (ARAC) synthetic dye as a substrate model. ARAC is a very persistent textile dye with established carcinogenic and toxic effects [40–42]. The sonication runs were conducted at 600 kHz using a standing wave reactor operating in continuous mode. The aims of the work are: (i) to investigate the possible activation of chlorine by power ultrasound at 600 kHz and 120 W, (ii) to demonstrate the synergistic effect of the US/chlorine process toward the degradation of ARAC, (iii) to propose a reaction mechanism for the sono-activation of chlorine and (iv) to study the influence of various processing conditions, i.e., pH, chlorine and ARAC concentrations, and the nature of saturating gases on the synergistic effect of the US/chlorine sono-hybrid process. To the best of our knowledge, no previous research has been conducted to explore the synergistic effect of US/chlorine toward the oxidation of organic pollutants in aqueous media, except our recent paper [39].

2. Results and Discussion

2.1. Aqueous Chlorine Chemistry and ARAC Chlorination Tests

In water treatment, gaseous chlorine (Cl_2) or hypochlorite are commonly used for chlorination processes. Chlorine gas (Cl_2) hydrolyzes in water according to the reaction [14]:

$$Cl_2 + H_2O \rightleftharpoons HOCl + H^+ + Cl^- \; K_{a1} = 3.94 \times 10^{-4}\ M^2 \text{ at } 25\ ^\circ C \text{ and } I = 0 \quad (5)$$

For a temperature range of 0–25 °C, K_{a1} ranges from 1.3×10^{-4} to 5.1×10^{-4} M^2 [35]. Hypochlorous acid (HOCl) resulting from Equation (5) is a weak acid, which dissociates in aqueous solution according to the reaction from Equation (6) [14]:

$$HOCl \rightleftharpoons OCl^- + H^+ \; pK_{a2} = 7.536 \; K_{a2} = 2.9 \times 10^{-8}\ M \text{ at } 25\ ^\circ C \text{ and } I = 0 \quad (6)$$

The K_{a2} value also depends on temperature, it varies between 1.5×10^{-8} M at 0 °C and 2.9×10^{-8} M at 25 °C. The distribution of free chlorine species depends on chloride concentration, temperature and pH; of all, pH is the most impactful parameter. Figure S1a (Supplementary Materials) shows the calculated distribution of Cl_2, HOCl and ClO^- as a function of pH at 25 °C and for a chloride concentration of 2 mM. At 25 °C, Cl_2 is only present at low pH values (pH < 3). HOCl is the predominant free chlorine species at pH < 7.5, and ClO^- at pH > 7.5. More than 98% of free chlorine is present as HOCl in the pH range of 2.5–6, and as ClO^- at pH > 9. Therefore, under typical water treatment conditions in the pH range 6–9, hypochlorous acid and hypochlorite are the main chlorine species. In addition to these major chlorine species, other chlorine intermediates such as Cl_3^- and Cl_2O can also be formed [15], but their concentrations are very low. HOCl and ClO^- absorb UV light at wavelengths ranging from 200 to 375 nm (Figure S1b, Supplementary Materials). Absorption spectrums show maximum absorption bands centered at 236 nm for HOCl (ε~$102 \pm 2\ M^{-1}\ cm^{-1}$) and at 294 nm for ClO^- (ε~$275 \pm 8\ M^{-1} \cdot cm^{-1}$).

The effect of an initial solution pH in the range of 1–10 on the direct chlorination of ARAC at 25 °C when using 250 μM of chlorine in continuously stirred (300 rpm) solutions was investigated in our previous work [39]. Additionally, the effect of chlorine dosage (50–300 μM) was also investigated at pH 5.5 [39]. Fast chlorination rates of the dye were observed in strong acidic and basic mediums [39]. Removals of 80% for pH 1 and 45% for pH 8–10 were achieved after 10 min of reaction, while 97%, 69% and 90% of the initial ARAC concentrations were eliminated after 40 min for pH 1, 8 and 10, respectively. However, very low removals of about 10–15% were obtained at pH 3–6 for up to 40 min of reaction. The dye molecules kept the same molecular form at pH 1–10 as the pK_a of the dye was 11.4 [43]. Therefore, ARAC reacts efficiently with Cl_2 (pH 1) and OCl^- (pH 8 and 10), whereas the dye molecules showed strong persistence toward the reaction with HOCl (pH 3–6), even at varying chlorine dosages [39]. Such pH dependence of chlorine reactivity has been previously reported for several organic and inorganic micropollutants such as triclosan, estrogenic steroid hormones, bisphenol A, acetaminophen, 4-n-nonylphenol and ammonia [35]. The oxidation potential of chlorine species is as follows: Cl_2 > HOCl > OCl^-. However, for a given compound, HOCl and ClO^- reactivities are usually significantly varied [35]. In addition, different species of the pollutant can be present in solution (i.e., depending on the pK_a of substrates). Therefore, pH dependence of the second-order rate constant is typically reported for chlorination reactions [35]. An important review on chlorine species reactivity toward a number of water contaminants is given by Deborde and Gunten [35]. The review illustrates some reaction mechanisms that take place during the chlorination of micropollutants.

2.2. Chlorine Sonolysis

The sonication of 250 μM chlorine aqueous solutions at 600 kHz and 120 W was conducted for pH 5 and 9. The recorded absorption spectrums during the sonolytic runs are plotted in Figure 1a,b. At pH 5, the HClO spectrum increases with time and its intensity becomes more important at higher irradiation times, particularly for $\lambda < \lambda_{max}$ = 236 nm. This trend reveals that the sonolysis of HClO may produce species that efficiently absorb UV light in the same band as that of HClO. These species may be characterized by higher molar absorption coefficients (ε) than that of HClO, which allows them to attain higher absorbance values even at lower concentration.

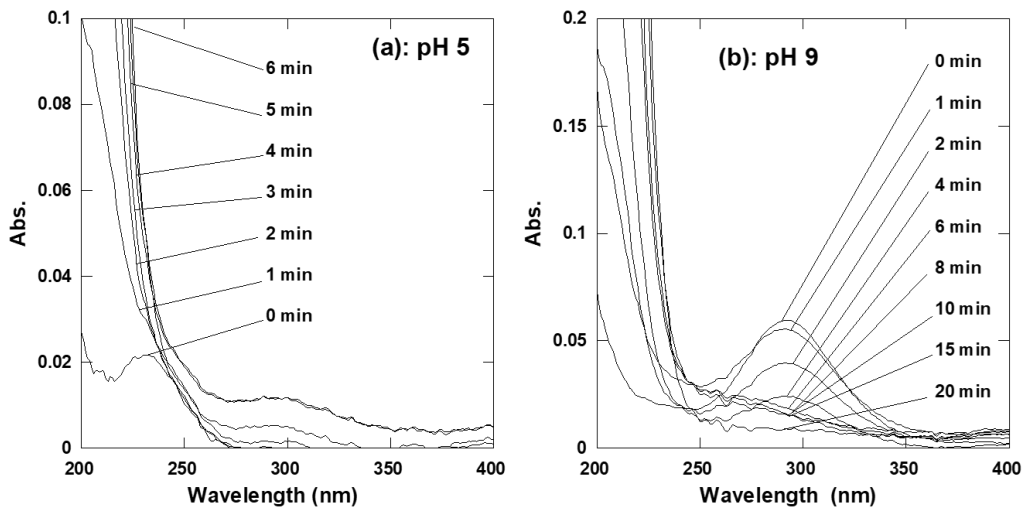

Figure 1. Chlorine sonolysis at pH 5 (**a**) and 9 (**b**) (conditions: $[chlorine]_0$ = 250 μM, V = 150 mL, temperature: 25 ± 1 °C, frequency: 600 kHz, power: 120 W).

However, chlorine decay upon sonolysis was clearly observed at pH 9 (Figure 1b). The pick intensity of OCl^- at 294 nm decreases progressively with time until it attains total disappearance at 20 min of irradiation; the trend was simultaneously accompanied by

quick growth of the absorption band, for which λ < 240 nm, which can confirm the above suggestion concerning the high molar absorption coefficients (ε) of chlorine sono-products. Thus, it can be concluded that the product of ClO^- sonolysis does not absorb UV light in the same region as that of hypochlorite. Chlorine was presumably degraded via a radical pathway in which chlorine species initially react with the acoustically generated reactive species ($^{\bullet}OH$, $H^{\bullet}$, $HO_2^{\bullet}$ and H_2O_2). The following reaction mechanism (Equations (7)–(32)) including initiation [14,15,17,44], propagation [14,15,22,45] and termination reactions [14,46] (all involved in UV/chlorine AOP [14,15,17]) is postulated for a pH range of 1–10:

$$\text{Initiation: } HO_2^{\bullet} \rightarrow O_2^{\bullet -} + H^+ \quad pK_a = 4.7 \tag{7}$$

$$^{\bullet}OH + HClO \rightarrow ClO^{\bullet} + H_2O \quad k_8 = 2 \times 10^9\ M^{-1}\ s^{-1} \tag{8}$$

$$^{\bullet}OH + ClO^- \rightarrow ClO^{\bullet} + OH^- \quad k_9 = 9.8 \times 10^9\ M^{-1}\ s^{-1} \tag{9}$$

$$^{\bullet}H + HClO \rightarrow {}^{\bullet}OH + HCl \quad k_{10} = 5 \times 10^8\ M^{-1}\ s^{-1} \tag{10}$$

$$^{\bullet}H + HClO \rightarrow Cl^{\bullet} + H_2O \quad k_{11} = 5 \times 10^8\ M^{-1}\ s^{-1} \tag{11}$$

$$^{\bullet}H + HClO \rightarrow ClO^{\bullet} + H_2 \quad k_{12} = 5 \times 10^8\ M^{-1}\ s^{-1} \tag{12}$$

$$HO_2^{\bullet}/O_2^{\bullet -} + HClO \rightarrow Cl^{\bullet} + O_2 + H_2O/OH^- \quad k_{13} = 7.5 \times 10^6\ M^{-1}\ s^{-1} \tag{13}$$

$$H_2O_2 + HClO \rightarrow HCl + O_2 + H_2O \quad k_{14} = 1.1 \times 10^4\ M^{-1}\ s^{-1} \tag{14}$$

$$H_2O_2 + ClO^- \rightarrow Cl^- + O_2 + H_2O \quad k_{15} = 1.7 \times 10^5\ M^{-1}\ s^{-1} \tag{15}$$

$$\text{Propagation: } HCl \rightleftharpoons H^+ + Cl^- \quad pK_a = -6.3 \tag{16}$$

$$Cl^{\bullet} + HClO \rightarrow ClO^{\bullet} + H^+ + Cl^- \quad k_{17} = 3 \times 10^9\ M^{-1}\ s^{-1} \tag{17}$$

$$Cl^{\bullet} + ClO^- \rightarrow ClO^{\bullet} + Cl^- \quad k_{18} = 8.2 \times 10^9\ M^{-1}\ s^{-1} \tag{18}$$

$$Cl^{\bullet} + H_2O \rightarrow HClO^{\bullet -} + H^+ \quad k_{19} = 2.5 \times 10^5\ s^{-1} \tag{19}$$

$$Cl^{\bullet} + OH^- \rightarrow HClO^{\bullet -} \quad k_{20} = 1.8 \times 10^{10}\ M^{-1}\ s^{-1} \tag{20}$$

$$HClO^{\bullet -} \rightleftharpoons {}^{\bullet}OH + Cl^- \quad k_{21} = 6.9 \times 10^9\ M^{-1}\ s^{-1} \tag{21}$$

$$HClO^{\bullet -} + H^+ \rightarrow Cl^{\bullet} + H_2O \quad k_{22} = 2.1 \times 10^{10}\ M^{-1}\ s^{-1} \tag{22}$$

$$HClO^{\bullet -} + Cl^- \rightarrow Cl_2^{\bullet -} + OH^- \quad k_{23} = 1 \times 10^5\ M^{-1}\ s^{-1} \tag{23}$$

$$Cl^{\bullet} + Cl^- \rightleftharpoons Cl_2^{\bullet -} \quad k_{24} = 8.5 \times 10^9\ M^{-1}\ s^{-1} \tag{24}$$

$$Cl_2^{\bullet -} + H_2O \rightarrow Cl^- + HClO^{\bullet -} + H^+ \quad k_{25} = 1 \times 10^5\ M^{-1}\ s^{-1} \tag{25}$$

$$Cl_2^{\bullet -} + OH^- \rightarrow Cl^- + HClO^{\bullet -} \quad k_{26} = 1 \times 10^5\ M^{-1}\ s^{-1} \tag{26}$$

$$\text{Termination: } Cl_2^{\bullet -} + {}^{\bullet}OH \rightarrow HClO + Cl^- \quad k_{27} = 1 \times 10^9\ M^{-1}\ s^{-1} \tag{27}$$

$$Cl_2^{\bullet -} + Cl^{\bullet} \rightarrow Cl_2 + Cl^- \quad k_{28} = 2.1 \times 10^9\ M^{-1}\ s^{-1} \tag{28}$$

$$^{\bullet}OH + {}^{\bullet}OH \rightarrow H_2O_2 \quad k_{29} = 5.5 \times 10^9\ M^{-1}\ s^{-1} \tag{29}$$

$$Cl^{\bullet} + Cl^{\bullet} \rightarrow Cl_2 \quad k_{30} = 8.8 \times 10^7\ M^{-1}\ s^{-1} \tag{30}$$

$$Cl_2^{\bullet -} + Cl_2^{\bullet -} \rightarrow Cl_2 + 2Cl^- \quad k_{31} = 6.3 \times 10^8\ M^{-1}\ s^{-1} \tag{31}$$

$$ClO^{\bullet} + ClO^{\bullet} \rightarrow Cl_2O_2 \quad k_{32} = 7.5 \times 10^9\ M^{-1}\ s^{-1} \tag{32}$$

Therefore, the sonolysis of chlorine can produce a number of highly reactive chlorine species (RCSs), i.e., mainly $Cl^{\bullet}$, $ClO^{\bullet}$ and $Cl_2^{\bullet -}$, which can be used for intensifying the degradation of water contaminants in a similar manner to that reported for UV/chlorine AOP.

2.3. Synergism of Coupling Ultrasound and Chlorine Treatments

Figure 2 shows the degradation kinetics of ARAC at 25 °C via the ultrasound (US: 600 kHz, 120 kHz), chlorine and US/chlorine processes for C_0 = 5 mg·L^{-1} (10 μM), [chlorine]$_0$ = 250 μM and a natural pH of 5.5. As clearly seen, removals of 10% and 50% were obtained after 10 min with, respectively, chlorine and US separately, whereas the US/chlorine combination ensured 92% removal at this time (i.e., 1.84- and 9.2-fold increases in chlorine and US yields separately). After 30 min, the ARAC was removed at 99%, compared to 15% and 70% for, respectively, chlorination alone and sonolysis lone. The initial rate of ARAC removal (r_0) was 0.8 mg·L^{-1}·min^{-1} for the US/chlorine treatment compared to 0.35 mg·L^{-1}·min^{-1} for US and 0.1 mg·L^{-1}·min^{-1} for chlorine oxidation, yielding an $r_{0,US/chlorine}/r_{0,US}$ ratio of 2.28 and a synergy index SI = $r_{0,US/chlorine}/(r_{0,US} + r_{0,chlorine})$ equal to 1.74.

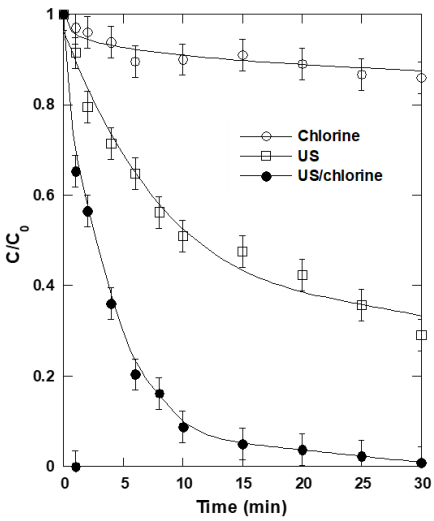

Figure 2. ARAC degradation kinetics via chlorine, ultrasound (US) and US/chlorine processes (conditions: C_0 = 5 mg·L^{-1} (10 μM), [chlorine]$_0$ = 250 μM, V = 150 mL, pH 5.5, temperature: 25 ± 1 °C, frequency: 600 kHz, power: 120 W).

The change in UV-Vis spectrums with time during the treatment of ARAC with the US and US/chlorine processes is shown in Figure 3a,b. For both processes, the abatement of the visible band of the chromophoric group is associated with (i) a decrease in the UV band at λ_{max} = 315 nm, which represents the absorptivity of the naphthenic group, and (ii) a rapid increase in the UV band for which λ_{max} < 250 nm (i.e., the absorption zone of the degradation by-products). This means that there is effective destruction of the dye molecules, and not only a decolorization process. However, the abatement rate of the UV-315 nm band is too rapid for the US/chlorine process compared to sole sonication. In fact, this band completely disappeared after 40 min under the sono-chlorination process compared to 100 min US. The initial rates of absorbance abatement at λ_{max} = 315 nm are 4.64 × 10^{-3} min^{-1} for US/chlorine and 1.21 × 10^{-3} min^{-1} for US, which provides a ratio of 3.83 (i.e., no change in absorbance at λ_{max} = 315 nm was recorded with the chlorine treatment). Thus, the synergistic effect of the US/chlorine system is more efficient for aromatic ring destruction than ARAC decolorization.

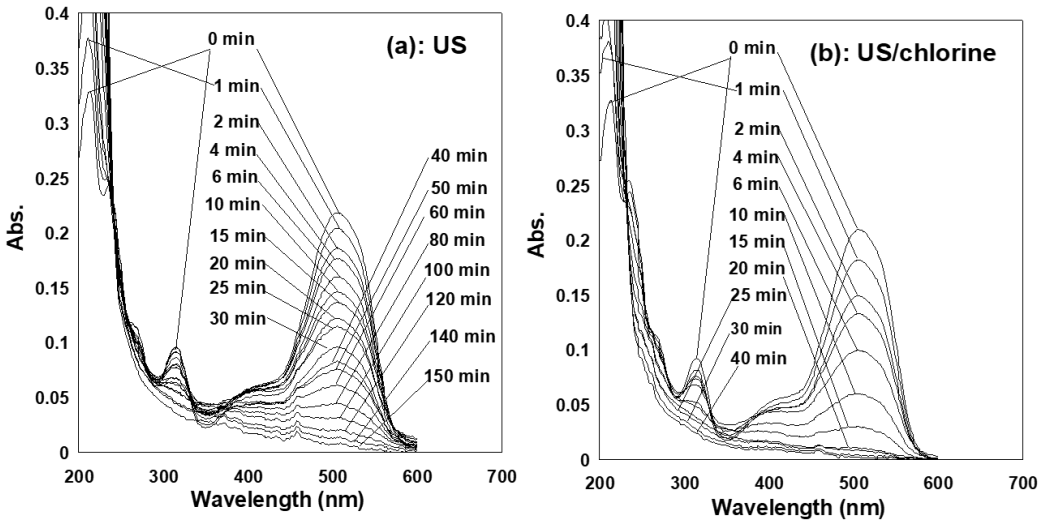

Figure 3. Changes in UV-Vis spectrums during the treatment of ARAC via ultrasound (US) (**a**) and US/chlorine (**b**) processes (conditions: C_0 = 5 mg·L^{-1} (10 μM), [chlorine]$_0$ = 250 μM, V = 150 mL, pH 5.5, temperature: 25 ± 1 °C, frequency: 600 kHz, power: 120 W).

2.4. Source of the Synergistic Effect

Firstly, ARAC is a highly hydrophilic water solute (solubility: 225 g·L^{-1}, log K_{ow} = −0.55 [47]) of negligible volatility. Thus, ARAC cannot enter the bubbles during the sonolytic treatment but must be degraded outside the bubbles by a reaction with the $^{\bullet}$OH radical ejected from inside the bubbles. This degradation pathway has been confirmed by the addition of nitrobenzene (NB) as a selective scavenger of $^{\bullet}$OH ($k_{NB,^{\bullet}OH}$ = 3.9 × 10^9 [15]). ARAC removal was inhibited by more than 90% when NB was added at 1 mM [39]. Moreover, H_2O_2 analysis demonstrated the dominance of an $^{\bullet}$OH attack on ARAC molecules at the bubble/solution interface [39]. H_2O_2 is mainly formed at the bubble/solution interface via 2$^{\bullet}$OH → H_2O_2 (k = 5.5 × 10^9 M^{-1}·s^{-1}) [48,49]. The rate of hydrogen peroxide formation decreased from 5.6 μM·min^{-1} in pure water to 4.17 μM·min^{-1} in ARAC aqueous solution (5 mg·L^{-1}), meaning that ARAC molecules scavenge an appreciable portion of hydroxyl radicals located at the reactive interfacial region. Consequently, the sono-degradation of ARAC mainly takes place at the bubble/solution interface, but some degradation reactions can also occur in the bulk solution since NB addition in excess ([NB]$_0$/[ARAC]$_0$ = 100 at 1 mM NB) does not completely quench the dye degradation [39]. In fact, it is reported that ~10% of the formed $^{\bullet}$OH in the bubble can achieve the solution bulk (i.e., the concentration of radicals is higher at the bubble/solution interface) [12,50].

Therefore, the synergism resulting from the application of the US/chlorine process was attributed to the sonolytic activation of chlorine (Equations (7)–(32)). Acoustically generated reactive species ($^{\bullet}$OH, H$^{\bullet}$, $HO_2^{\bullet}$ and H_2O_2) can react with HClO/ClO$^-$ to produce RCSs (Cl$^{\bullet}$, ClO$^{\bullet}$ and $Cl_2^{\bullet-}$) that work together with $^{\bullet}$OH to quickly destroy the dye molecules. The overall degradation event mostly takes place at the bubble/solution interface where the maximum concentration of reactive species is present. However, RCSs were characterized by a longer lifetime than that of $^{\bullet}$OH, i.e., 5 μs for Cl$^{\bullet}$ [34] and fractions of milliseconds for $Cl_2^{\bullet-}$ [34], revealing that RCSs have enough time to diffuse far from the bubble interface towards the solution bulk and react with ARAC molecules.

Consequently, ARAC degradation in the US/chlorine system may also happen in the bulk of the solution. Thus, the US/chlorine process could be promising for the degradation of hydrophilic pollutants.

2.5. Synergism Dependence of Chlorine Dosage

Figure 4 shows the effect of an initial chlorine dosage in the range of 50–300 μM on the removal kinetics of ARAC (C_0 = 5 mg·L^{-1}) via the US/chlorine combination at 25 °C and pH 5.5. The removal rate of the dye increased rapidly with increasing [chlorine]$_0$. The ARAC removal efficiency after 6 min increased from 35% for US alone to 63%, 68%, 80% and 100% when chlorine was added at 100, 200, 250 and 300 μM, respectively. Chlorination alone removed at maximum 10–15% of ARAC for all investigated [chlorine]$_0$ [39]. The initial rate of ARAC removal (r_0) increased from 0.35 mg·L^{-1}·min^{-1} for US alone to 0.51, 0.70, 0.74, 0.80 and 1.01 mg·L^{-1}·min^{-1} for US/chlorine in the presence of 50, 100, 200, 250 and 300 μM of chlorine, respectively, yielding an increasing $r_{0,US/chlorine}/r_{0,US}$ ratio of 1.44 at [chlorine]$_0$ = 50 μM, 2 at [chlorine]$_0$ = 100 and 200 μM, 2.23 at [chlorine]$_0$ = 250 μM and 2.83 at [chlorine]$_0$ = 300 μM. Using a maximum elimination rate of 0.1 mg·L^{-1}·min^{-1} for the chlorination alone, the synergy index SI = $r_{0,US/chlorine}/(r_{0,US} + r_{0,chlorine})$ increased from 1.13 for [chlorine]$_0$ = 50 μM to 1.56 for [chlorine]$_0$ = 100 μM, 1.64 for [chlorine]$_0$ = 200 μM, 1.74 for [chlorine]$_0$ = 250 μM and 2.24 for [chlorine]$_0$ = 300 μM, respectively.

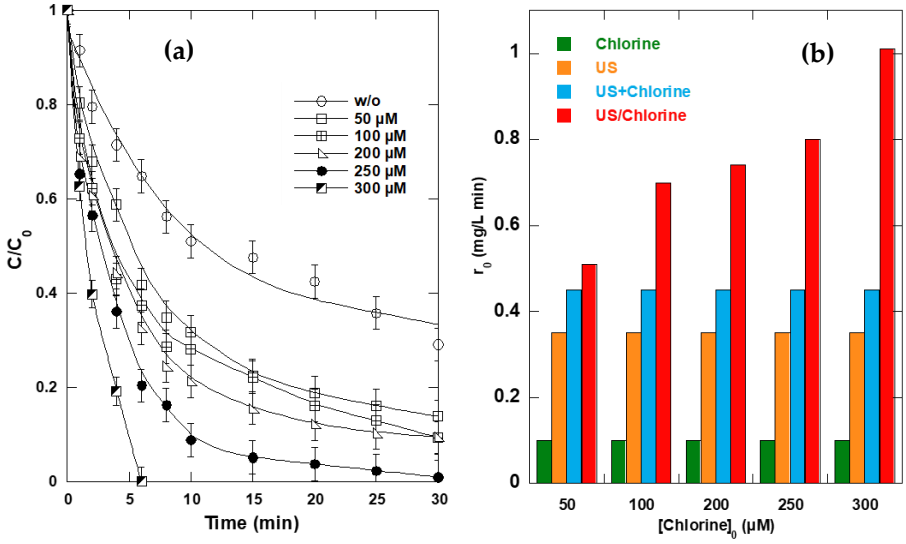

Figure 4. Effect of initial chlorine concentration on the sonochemical degradation of ARAC (**a**) (conditions: C_0 = 5 mg·L^{-1} (10 μM), [chlorine]$_0$ = 50–300 μM, V = 150 mL, pH 5.5, temperature: 25 ± 1 °C, frequency: 600 kHz, power: 120 W) and variation in initial ARAC removal rate (r_0) with respect to [chlorine]$_0$ for chlorination alone, US alone and US/chlorine combination (**b**) (the sum of the two processes separately, US + chlorine, was added for comparison with the combined process).

Therefore, the synergistic effect increases with increasing initial chlorine dosage without the observation of an optimum SI, as reported recently in the case of the UV/chlorine process [20,51,52]. It can therefore be concluded that increasing chlorine concentration in the solution could result in a higher concentration of RCSs ($Cl^{\bullet}$, $ClO^{\bullet}$ and $Cl_2^{\bullet-}$), thereby increasing the dye removal. The absence of an optimum was simply attributed to the fact that the required chlorine concentration, which quenches the beneficial effect of chlorine toward RCS generation and use, has not been attained.

2.6. Synergism Dependence of pH

The effect of varying the initial solution pH from 1 to 10 on the ARAC (C_0 = 5 mg·L^{-1}) removal kinetics via the US and US/chlorine processes is given in Figure 5 for an initial chlorine concentration of 250 μM. For both systems, the solution pH in the interval of 4 to 10 did not affect the degradation rate of the dye, but higher rates were obtained at pH 1 using ultrasound alone. However, the US/chlorine process ensured much higher degradation efficiency than sonication alone over the whole investigated range of pH values. A higher syn-

ergy index of 1.74 was always maintained for pH 4–6 (i.e., $r_{0,US/chlorine}$ ~ 0.8 mg·L^{-1}·min^{-1}, $r_{0,US}$~0.35 mg·L^{-1}·min^{-1}, $r_{0,chlorine}$~0.1 mg·L^{-1}·min^{-1}) where chlorination alone did not significantly affect the degradation of the dye [39]. At pH 1 and pH 8–10, ARAC chlorination happed at appreciable initial rates of 0.54 and 0.41 mg·L^{-1}·min^{-1}, respectively [39]. Additionally, the sonolytic degradation of ARAC in strong acidic medium (pH 1) was as high as that ensured by chlorination alone (0.832 mg·L^{-1}·min^{-1}), with the same r_0 obtained for the US/chlorine process. Therefore, the synergistic effect of the US/chlorine process was negative at pH 1 (SI = 0.6 < 1); the dye destruction in this case was predominately controlled by sonication alone rather than the coupled system. For pH 8 and 10, the effect of applying US/chlorine was additive as the synergistic index was equal to 1 (i.e., $r_{0,US/chlorine}$~0.8 mg·L^{-1}·min^{-1}, $r_{0,US}$~0.35 mg·L^{-1}·min^{-1}, $r_{0,chlorine}$~0.41 mg·L^{-1}·min^{-1}). Therefore, the synergism of applying US/chlorine treatment was obtained at pH 4−6, where HOCl is the sole chlorine species.

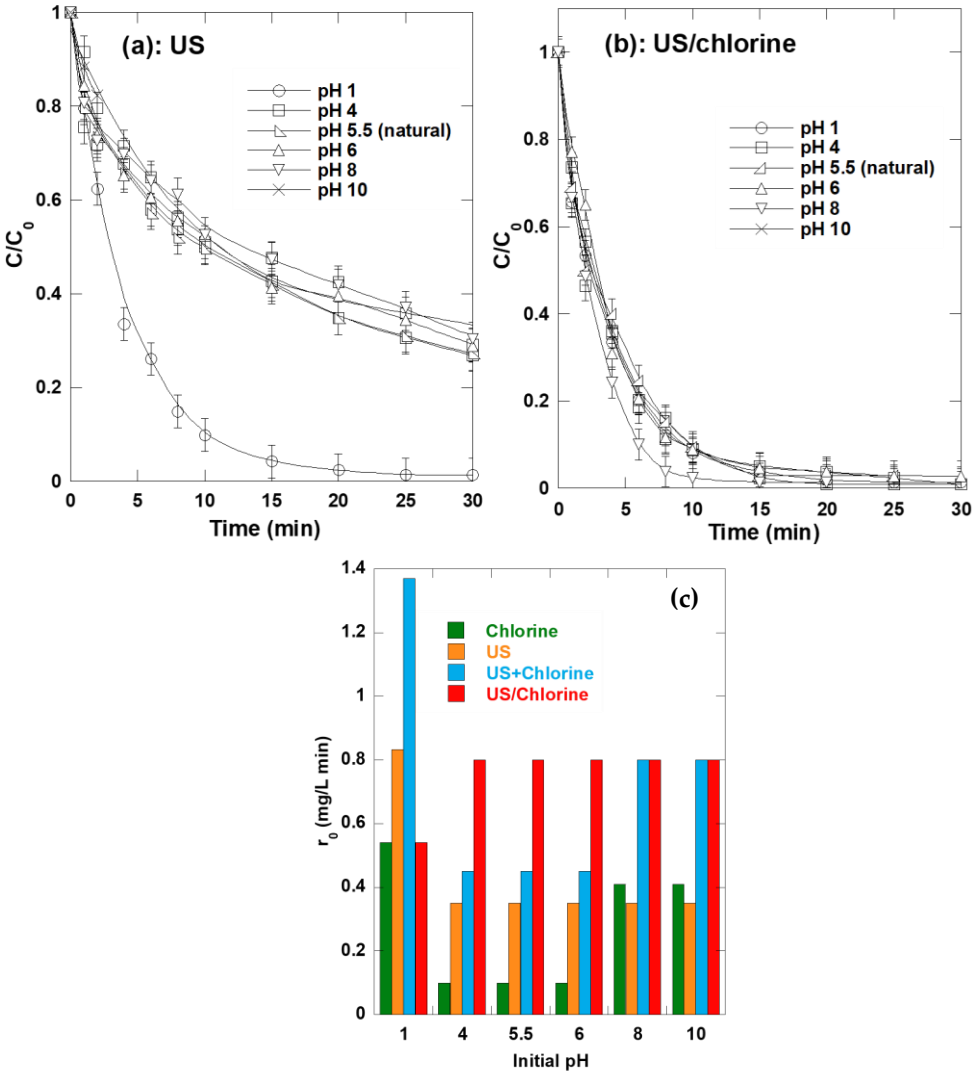

Figure 5. Effect of initial solution pH on the performance of US (**a**) and US/chlorine (**b**) processes toward the removal kinetics of ARAC (conditions: C_0 = 5 mg·L^{-1} (10 μM), [chlorine]$_0$ = 250 μM, V = 150 mL, pH 1–10, temperature: 25 ± 1 °C, frequency: 600 kHz, power: 120 W) and variation in ARAC initial removal rate (r_0) with respect to initial solution pH for chlorination alone, US alone and US/chlorine combination (**c**) (the sum of the two processes separately, US + chlorine, was added for comparison with the combined process).

In sonochemical treatments, the solution pH affects substrate ionization/protonation depending on their dissociation pK_a. Ionizable substrates are more hydrophilic than the protonated ones. They preferentially stay in the bulk solution, particularly at low concentrations, but their hydrophobicity increases when the protonated form is dominated. Because the pK_a of ARAC is 11.4 [43], the dye molecule can maintain the same form up to pH 10; therefore, dye sonolysis cannot be affected by pH elevation up to 10, as stated in Figure 5a. However, the strong acidic medium (pH 1) can protonate the two sulfonate groups ($-SO_3^-$) of the dye, which increases the dye hydrophobicity and accumulation at the reactive bubble/solution interface where the concentration of $^{\bullet}OH$ is at a higher level [53]. The degradation rate at pH 1 could therefore be more appreciable than under neutral and alkaline conditions. Additionally, the concentration of the dissolved CO_2 gas, i.e., from the atmosphere, in the solution is much higher at acidic conditions (i.e., at neutral and basic mediums, HCO_3^- and CO_3^{2-} are the most abundant acid carbonic forms). It has been reported that the injection of CO_2 at low concentration improves sonochemical treatment by increasing the number of active bubbles, i.e., since CO_2 could provide more nucleation sites for cavitation [54–56]. A detailed report on how CO_2 affects sonochemical efficiency was recently provided by Merouani et al. [57]. Therefore, the CO_2-impoving cavitation event is another reason for the higher degradation extent of ARAC at pH 1. The same reason for the effect of pH 1 was maintained for the US/chlorine system, as the overall degradation rate is controlled by the sonolytic process, as stated earlier. For pH 4–6, the synergistic degradation rate is constant as HOCl is the sole chlorine species at pH 4–6 (Figure S1a, Supplementary Materials). For pH 8–10, the combined effect of US and chlorine is additive, and consequently, there is no need for it to be discussed.

2.7. Synergism Dependence of Saturating Gases

Figure 6 shows the effect of three saturating gases (argon, air and nitrogen) on ARAC degradation kinetics via US treatment and the US/chlorine process in the presence of 250 μM of chlorine. It is observed that the US/chlorine system provided the best degradation rates for the three gas atmospheres. For the US treatment, the degradation efficiency follows the order Ar > air > N_2, whereas the order for the US/chlorine system is air > Ar > N_2. Initial degradation rates (r_0) of 0.43 $mg \cdot L^{-1} \cdot min^{-1}$ for Ar, 0.35 $mg \cdot L^{-1} \cdot min^{-1}$ for air and 0.137 $mg \cdot L^{-1} \cdot min^{-1}$ for N_2 were recorded for the ultrasonic treatment. Chlorine engenders an increase in the initial degradation rates by 30%, 128% and 37% for, respectively, for argon, air and N_2 saturations. The calculated synergy indexes are 1.1 for Ar, 1.74 for air and 0.8 for N_2 (i.e., for all gases, $r_{0,chlorine}$ = 0.1 $mg \cdot L^{-1} \cdot min^{-1}$). Therefore, the effect of combining US and chlorine for ARAC degradation is additive for argon, synergistic for air and negative for N_2.

The obtained order of the saturating gases (Ar > air > N_2) for the US process is largely reported in the literature [58–61]. The measured accumulation rate of H_2O_2 in water, as $^{\bullet}OH$ quantifiers, were 6.4 $\mu M \cdot min^{-1}$ for Ar, 5.6 $\mu M \cdot min^{-1}$ for air and 3 $\mu M \cdot min^{-1}$ for N_2. Therefore, a higher production rate of hydroxyl radicals was associated with argon, then to air and, finally, to N_2. An interesting numerical investigation of how these gases affect the sonochemical activity was recently provided by Merouani et al. [9,62]. Overall, thanks to its beneficial physical properties (i.e., a greater polytropic ratio (γ_{Ar} = 1.66) and solubility ($x_{Ar} = 2.748 \times 10^{-5}$) and lower thermal conductivity (λ_{Ar} = 0.018 W $m^{-2} \cdot K^{-1}$) than air and N_2 gases, which have the same γ and λ (γ = 1.41, λ = 0.026 W $m^{-2} \cdot K^{-1}$) and a slight differences in their solubility ($x_{air} = 1.524 \times 10^{-5}$, $x_{N2} = 1.276 \times 10^{-5}$)), argon could produce the highest single-bubble yield ($^{\bullet}OH$ radical) and a greater number of bubbles than the other gases [60,63,64], allowing it to achieve the maximum sonochemical efficiency. The higher chemical efficiency in air-saturated solution than N_2 was mainly attributed to the internal bubble-chemistry [9,62]. The presence of a high N_2 concentration inside the bubble at the collapse decreased the production rate of radicals [9,62]. The reason for this trend was associated with the consumption of $^{\bullet}OH$ radicals through the reaction $NO + {}^{\bullet}OH + M \leftrightarrow HNO_2 + M$. Consequently, because oxidizing nitrogen NO is formed

mainly, as found, through the reactions $N_2 + O \rightleftharpoons NO + N$ and $NO_2 + M \rightleftharpoons O + NO + M$, the higher the concentration of N_2 in the bubble, the higher the concentration of NO will be; this accelerates the consumption rate of $^{\bullet}OH$ radicals through the reaction $NO + {}^{\bullet}OH + M \rightleftharpoons HNO_2 + M$ [9,62]. Therefore, air could yield higher sonochemical efficiency than an N_2 atmosphere.

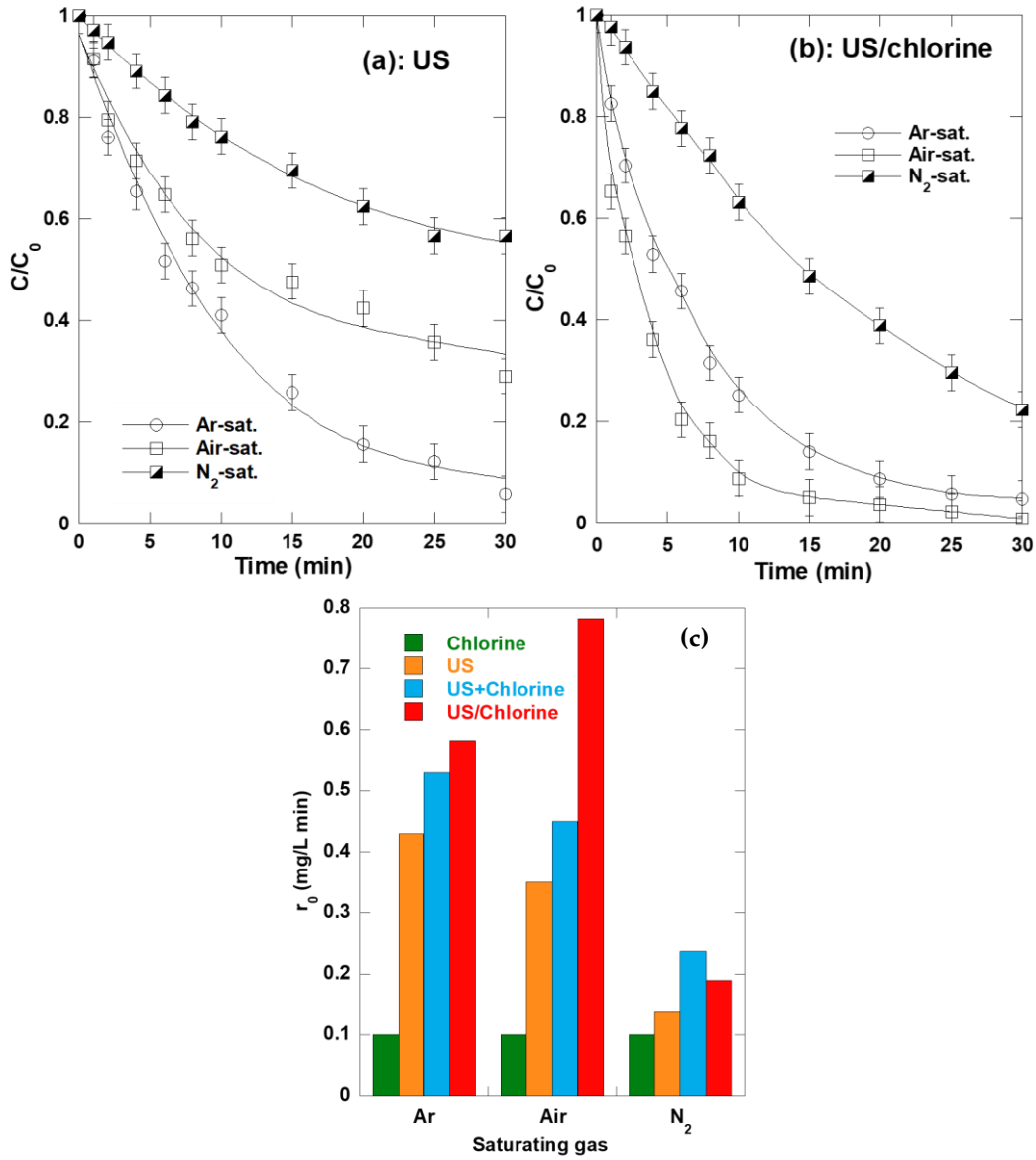

Figure 6. Effect of saturation gases on the performance of US (**a**) and US/chlorine (**b**) processes toward the removal kinetics of ARAC (conditions: C_0 = 5 mg·L^{-1} (10 μM), $[chlorine]_0$ = 250 μM, V = 150 mL, pH 5.5, temperature: 25 ± 1 °C, frequency: 600 kHz, power: 120 W) and variation in ARAC initial removal rate (r_0) with respect to saturating gas for chlorination alone, US alone and US/chlorine combination (**c**) (the sum of the two processes separately, US + chlorine, was added for comparison with the combined process).

For the US/chlorine system, the resulting negative synergy under a nitrogen saturation atmosphere was due to the poor production rate of the generated reactive species from the acoustic bubbles, as stated below. This could lower the production of RCSs, which are responsible for the synergistic effect. On the other hand, the absence of synergy under argon atmosphere was interpreted as follows: the radical–radical reactions, which are characterized by high second-order rate constants (Equations (27)–(32)), could always

accompany the radical–organic reactions. The radical–radical reaction was classified as a parasite reaction for organic degradation because they reduce the radicals' availability in the solution [16,20,65]. As argon ensures a higher concentration of reactive species (as quantified by H_2O_2 dosage), it may be that the generated concentration of RCSs is too high, which favors radicals quenching by themselves (Reactions (27)–(32)) rather than their reaction with the organic pollutant. Such scenarios are widely reported in the literature for several cases of AOPs [16,20,65–67]. Therefore, an air atmosphere could provide the best synergy as it generates a relatively moderate concentration of hydroxyl radicals, and therefore RCSs, as compared to argon, which marginalizes radical–radical reactions compared to radical–organic ones.

2.8. Synergism Dependence of Initial ARAC Concentration

Figure 7 depicts the effect of initial dye concentration (C_0 = 5–40 mg·L^{-1}) on the performance of US treatment and the US/chlorine process (250 μM of chlorine) at pH 5.5. Higher removal rates were associated with the US/chlorine process as compared to US alone for the four tested concentrations of C_0. After 10 min of reaction, US/chlorine eliminated 92%, 73%, 53%, 43% and 34% for C_0 = 5, 10, 20, 30 and 40 mg L^{-1}, respectively, compared to 50%, 38%, 31%, 30% and 36% for US alone. The elimination ratio between the two processes decreased from 1.84 for C_0 = 5 mg·L^{-1} to 1.7 and 1.48 for C_0 = 20 and 40 mg·L^{-1}, respectively. Correspondingly, the calculated synergistic index SI = $r_{0,US/chlorine}$/($r_{0,US}$ + $r_{0,chlorine}$) decreased from 1.74 for C_0 = 5 mg·L^{-1} to 1.46 for C_0 = 10 mg·L^{-1}, 1 for C_0 = 20 and 30 mg·L^{-1} and 0.8 for C_0 = 40 mg·L^{-1}. Therefore, the US/chlorine process is more synergistic at low dye concentrations. For higher concentrations, the process is not synergistic.

In sonochemical treatment, increasing the pollutant concentration in the solution bulk could increase its concentration at the reactive interfacial region [68,69]. Therefore, the higher the C_0, the higher the initial degradation rate could be. In fact, initial rates of 0.35, 0.57, 0.85, 1 and 1.36 mg·L^{-1}·min^{-1} were recorded for C_0 = 5, 10, 20, 30 and 40 mg·L^{-1}, respectively, in the absence of chlorine. This means that the scavenging of the acoustically generated hydroxyl radicals at the bubble/solution interface could be more efficient at a higher pollutant concentration. When chlorine is present, it creates strong competition with the pollutant substrate to react with the cavitation-generated reactive species. Increasing C_0 could reduce the fraction of the reactive species scavenged by chlorine, thereby decreasing the concentration of RCSs responsible for the synergistic action. Therefore, it is preferable to operate the US/chlorine process at a low pollutant concentration to maintain higher synergistic level.

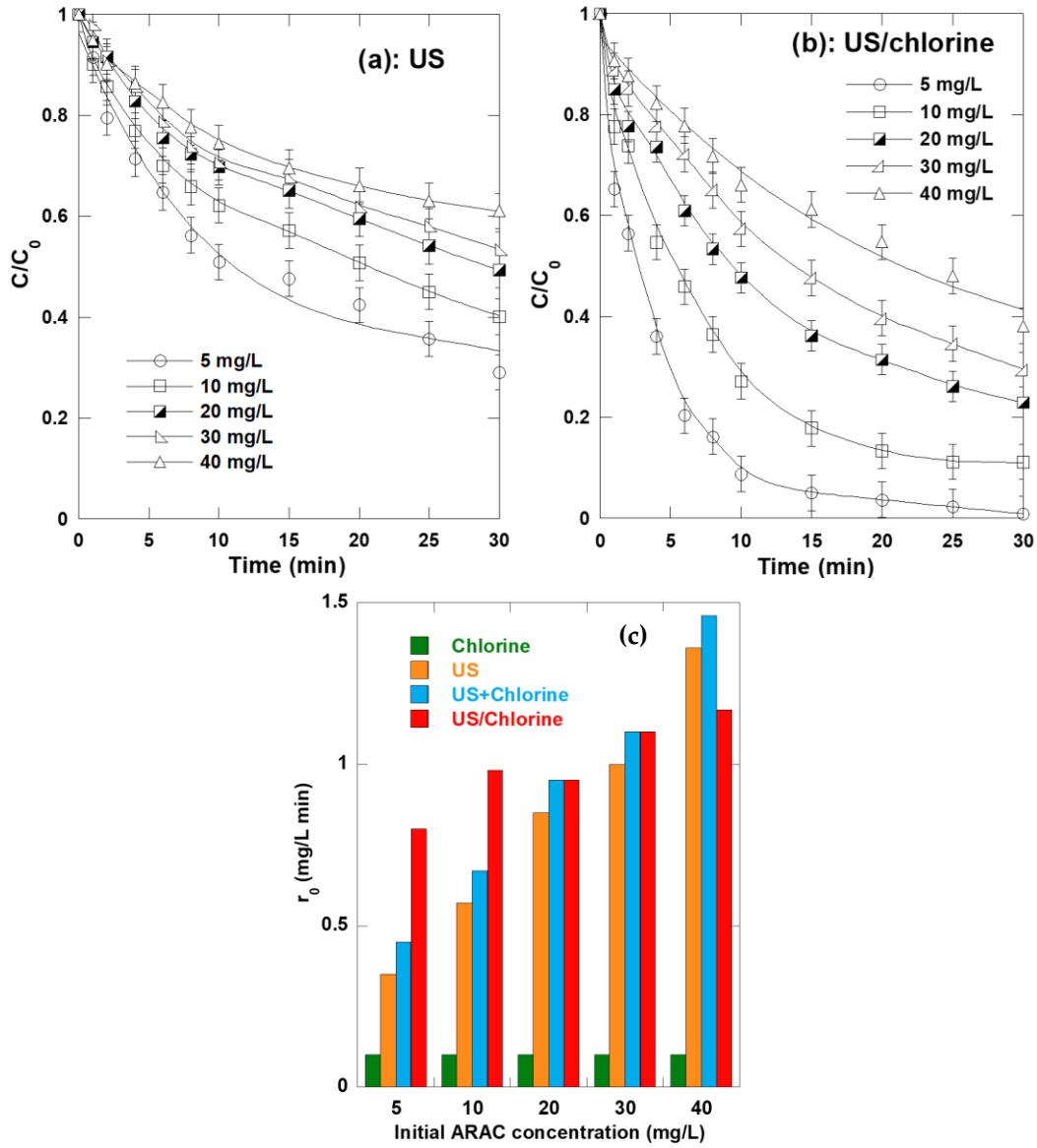

Figure 7. Effect of initial dye concentration on the performance of US (**a**) and US/chlorine (**b**) processes toward the removal kinetics of ARAC (conditions: C_0 = 5–40 mg·L^{-1} (10 μM), [chlorine]$_0$ = 250 μM, V = 150 mL, pH 5.5, temperature: 25 ± 1 °C, frequency: 600 kHz, power: 120 W) and variation in ARAC initial removal rate (r_0) with respect to initial de concentration for chlorination alone, US alone and US/chlorine combination (**c**) (the sum of the two processes separately, US + chlorine, was added for comparison with the combined process).

3. Materials and Methods

Throughout the study, ultrapure water was used for solution and sample preparation. Sodium hypochlorite solution (available active chlorine basis: ~16%) and Allura Red AC (abbreviation: ARAC; CAS number: 25956-17-6; chemical formula: $C_{18}H_{14}N_2Na_2O_8S_2$; molecular weight: 496,42 g·mol^{-1}) were supplied by Sigma-Aldrich (St. Louis, MO, USA). The molecular structure of ARAC is given in Figure S2. All other reagents (NaOH, H_2SO_4, KI, $(NH_4)_6Mo_7{\cdot}4H_2O$ and nitrobenzene) were commercial products of the purest grade available (Sigma-Aldrich).

Sonolytic runs were conducted using 150 mL of solution in the cylindrical water-jacketed glass reactor presented in Figure S3. The source of ultrasonic irradiation was a piezoelectric disc fixed on a stainless steel plate in the bottom of the reactor. US irradiation was emitted at a frequency of 600 kHz and at variable electric powers. For all experiments

in this study, the electric power delivered from the generator was fixed at 120 W. The temperature of the irradiating liquid was controlled through the cooling jacket and displayed using a thermocouple immersed in solution. The acoustic energy dissipated in the solution (~23 W) was estimated using the calorimetric method [49].

Stock solutions of chlorine (100 mM, pH 5) and ARAC (500 mg·L^{-1}, pH ~ 5.5) were prepared and stored in the dark at 4 °C. Experiments were carried out under different conditions at ambient temperature (25 ± 1 °C). The pH of the solution was adjusted using NaOH or H_2SO_4 (0.1 M). For the test of gases, each gas was bubbled 20 min prior to start and until completion of experiments. Quantitative analysis of the dye concentration was performed using Biochrom WPA Lightwave II UV-Vis. spectrophotometer at λ_{max} = 504 nm. Note that the variation in pH in the range of 1–10 affected neither λ_{max} nor the initial absorbance at λ_{max}. During sonication, hydrogen peroxide concentrations were quantified according to the iodometric method [49]. To ensure reproducibility of the results, all runs were performed in triplicate and results were presented as averages. Error bars, reported in the relevant data, represent the deviation of means.

4. Conclusions

Based on the obtained results, it can be concluded that the US/chlorine process could be more suitable to quickly abate persistent organic pollutants under typical water treatment conditions (air-equilibrated solution, pH 4–6, ambient temperature and low pollutant concentration). The process can generate reactive chlorine species, i.e., via the sonochemical activation of chlorine, which greatly improve the degradation rate of the pollutant. A synergistic index of 1.74 was obtained via the US/chlorine process for the degradation of ARAC (C_0 = 5 mg·L^{-1}) at pH 5.5 and $[chlorine]_0$ = 250 mM. The synergy index increased with increasing initial chlorine dosage without the observation of an optimum. The absence of an optimum was simply attributed to the fact that the required chlorine concentration, which quenches the beneficial effect of chlorine toward RCS generation and use, was not reached. Additionally, the synergetic effect was only obtained at pH 4–6, where HOCl is the sole chlorine species. At pH 8–10, the combined effect of US and chlorine was additive. Furthermore, the influence of combining US and chlorine for ARAC removal was additive for argon, synergetic for air and negative for nitrogen. An air atmosphere could provide the best synergy as it produces a relatively moderate concentration of reactive species as compared to argon, which marginalizes radical–radical reactions compared to radical–organic ones. The US/chlorine process was more synergetic for low dye concentrations ($C_0 \leq 10$ mg·L^{-1}); the coupling effect was additive for moderate concentrations (C_0~20–30 mg· L^{-1}) and negative for higher concentrations (>30 mg·L^{-1}).

The US/chlorine process could be involved as one novel AOP in wastewater treatment, although some specific analyses are still required. While the main objective of the current work was to explore the process performance in terms of pollutant removal, further investigations will be conducted for the sake of completeness, assessing the following issues:

- TOC, BOD_5 and toxicity evolutions;
- Radicals' identification and contribution to the overall degradation rate;
- The effect of processing conditions (e.g., pH, temperature, chlorine and pollutant concentrations) on radicals' distribution;
- The identification of degradation by-products because of the possible formation of toxic trihalomethanes;
- The reaction mechanism and scheme for ARAC degradation.

Supplementary Materials: The following supporting information can be downloaded at: https://www.mdpi.com/article/10.3390/catal12101171/s1. Figure S1. (a) Chlorine speciation in 0.5 mM total chlorine as function of pH and for a chloride concentration of 2 mM, and (b) molar absorption coefficients (ε) of HOCl (pH 5) and OCl^- (pH 9) as a function of wavelength; Figure S2. Molecular structure of Allura Red AC (ARAC); Figure S3. Photograph of the sonochemical reactor used for the sonolytic experiments. (a) 600 kHz ultrasonic transducer, (b) cylindrical jacketed glass cell, (c) sonicated solution, (d) inlet cooling water, (e) outlet cooling water, (f) thermocouple.

Author Contributions: O.H.: supervision, conceptualization, methodology, formal analysis, project administration, resources, funding acquisition, investigation, validation and writing—review and editing; S.M.: conceptualization, methodology, validation, writing—original draft preparation and writing—review and editing; H.C.B.: investigation, validation and writing—review and editing; M.A.I.: investigation, validation and writing—review and editing; H.F.: validation, methodology, resources and writing—review and editing; A.A.: validation and writing—review and editing. All authors have read and agreed to the published version of the manuscript.

Funding: This research received no external funding.

Data Availability Statement: Not applicable.

Conflicts of Interest: The authors declare no conflict of interest.

References

1. Boczkaj, G.; Fernandes, A. Wastewater treatment by means of advanced oxidation processes at basic pH conditions: A review. *Chem. Eng. J.* **2017**, *320*, 608–633. [CrossRef]
2. Kanakaraju, D.; Glass, B.D.; Oelgemöller, M. Advanced oxidation process-mediated removal of pharmaceuticals from water: A review. *J. Environ. Manag.* **2018**, *219*, 189–207. [CrossRef] [PubMed]
3. Ameta, S.; Ameta, R. *Advanced Oxidation Processes for Wastewater Treatment: Emerging Green Chemical Technology*; Elsevier Science: London, UK, 2018; ISBN 9780128105252.
4. Stefan, M.I. *Advanced Oxidation Processes for Water Treatment: Fundamentals and Applications*; IWA Publishing: London, UK, 2017.
5. Pétrier, C. The use of power ultrasound for water treatment. In *Power Ultrasonics: Applications of High-Intensity Ultrasound*; Gallego-Juarez, J.A., Graff, K., Eds.; Elsevier: Cambridge, MA, USA, 2015; pp. 939–963.
6. Suslick, K.S.; Flannigan, D.J. Inside a Collapsing Bubble: Sonoluminescence and the Conditions During Cavitation. *Annu. Rev. Phys. Chem.* **2008**, *59*, 659–683. [CrossRef] [PubMed]
7. Yasui, K.; Tuziuti, T.; Lee, J.; Kozuka, T.; Towata, A.; Iida, Y. The range of ambient radius for an active bubble in sonoluminescence and sonochemical reactions. *J. Chem. Phys.* **2008**, *128*, 184705. [CrossRef]
8. Yasui, K.; Tuziuti, T.; Kozuka, T.; Towata, A.; Iida, Y. Relationship between the bubble temperature and main oxidant created inside an air bubble under ultrasound. *J. Chem. Phys.* **2007**, *127*, 154502. [CrossRef]
9. Merouani, S.; Hamdaoui, O.; Rezgui, Y.; Guemini, M. Sensitivity of free radicals production in acoustically driven bubble to the ultrasonic frequency and nature of dissolved gases. *Ultrason. Sonochem.* **2015**, *22*, 41–50. [CrossRef]
10. Makino, K.; Mossoba, M.M.; Riesz, P. Chemical effects of ultrasound on aqueous solutions. Evidence for $^{\bullet}OH$ an $^{\bullet}H$ by spin trapping. *J. Am. Chem. Soc.* **1982**, *104*, 3537–3539. [CrossRef]
11. Hart, E.J.; Henglein, A. Sonochemistry of aqueous solutions: H_2-O_2 combustion in cavitation bubbles. *J. Phys. Chem.* **1987**, *91*, 3654–3656. [CrossRef]
12. Henglein, A. Chemical effects of continuous and pulsed ultrasound in aqueous solutions. *Ultrason. Sonochem.* **1995**, *2*, 115–121. [CrossRef]
13. Thompson, L.H.; Doraiswamy, L.K. Sonochemistry: Science and Engineering. *Ind. Eng. Chem. Res.* **1999**, *38*, 1215–1249. [CrossRef]
14. Laat, J.D.E.; Stefan, M. UV/chlorine process. In *Advanced Oxidation Processes for Water Treatment*; Stefan, M.I., Ed.; IWA Publishing: London, UK, 2017; pp. 383–428.
15. Remucal, C.K.; Manley, D. Emerging investigators series: The efficacy of chlorine photolysis as an advanced oxidation process for drinking water treatment. *Environ. Sci. Water Res. Technol.* **2016**, *2*, 565–579. [CrossRef]
16. Meghlaoui, F.Z.; Merouani, S.; Hamdaoui, O.; Bouhelassa, M.; Ashokkumar, M. Rapid catalytic degradation of refractory textile dyes in Fe (II)/chlorine system at near neutral pH: Radical mechanism involving chlorine radical anion ($Cl_2^{\bullet-}$)-mediated transformation pathways and impact of environmental matrices. *Sep. Purif. Technol.* **2019**, *227*, 115685. [CrossRef]
17. Bulman, D.M.; Mezyk, S.P.; Remucal, C.K. The Impact of pH and Irradiation Wavelength on the Production of Reactive Oxidants during Chlorine Photolysis. *Environ. Sci. Technol.* **2019**, *53*, 4450–4459. [CrossRef] [PubMed]
18. Behin, J.; Akbari, A.; Mahmoudi, M.; Khajeh, M. Sodium hypochlorite as an alternative to hydrogen peroxide in Fenton process for industrial scale. *Water Res.* **2017**, *121*, 120–128. [CrossRef]

19. Meghlaoui, F.Z.; Merouani, S.; Hamdaoui, O.; Alghyamah, A.; Bouhelassa, M.; Ashokkumar, M. Fe(III)-catalyzed degradation of persistent textile dyes by chlorine at slightly acidic conditions: The crucial role of $Cl_2^{\bullet-}$ radical in the degradation process and impacts of mineral and organic competitors. *Asia-Pacific J. Chem. Eng.* **2020**, *16*, e2553. [CrossRef]
20. Belghit, A.; Merouani, S.; Hamdaoui, O.; Alghyamah, A.; Bouhelassa, M. Influence of processing conditions on the synergism between UV irradiation and chlorine toward the degradation of refractory organic pollutants in UV/chlorine advanced oxidation system. *Sci. Total Environ.* **2020**, *736*, 139623. [CrossRef]
21. Wang, W.L.; Wu, Q.Y.; Huang, N.; Wang, T.; Hu, H.Y. Synergistic effect between UV and chlorine (UV/chlorine) on the degradation of carbamazepine: Influence factors and radical species. *Water Res.* **2016**, *98*, 190–198. [CrossRef]
22. Fang, J.; Fu, Y.; Shang, C. The roles of reactive species in micropollutant degradation in the UV/free chlorine system. *Environ. Sci. Technol.* **2014**, *48*, 1859–1868. [CrossRef]
23. Wang, W.; Zhang, X.; Wu, Q.; Du, Y.; Hu, H. Degradation of natural organic matter by UV/chlorine oxidation: Molecular decomposition, formation of oxidation byproducts and cytotoxicity. *Water Res.* **2017**, *124*, 251–258. [CrossRef]
24. Wang, A.; Lin, Y.; Xu, B.; Hu, C.; Xia, S.; Zhang, T.; Chu, W. Kinetics and modeling of iodoform degradation during UV/chlorine advanced oxidation process. *Chem. Eng. J.* **2017**, *323*, 312–319. [CrossRef]
25. Kong, X.; Wu, Z.; Ren, Z.; Guo, K.; Hou, S.; Hua, Z.; Li, X.; Fang, J. Degradation of lipid regulators by the UV/chlorine process: Radical mechanisms, chlorine oxide radical ($ClO^{\bullet}$)-mediated transformation pathways and toxicity changes. *Water Res.* **2018**, *137*, 242–250. [CrossRef] [PubMed]
26. Xiang, Y.; Fang, J.; Shang, C. Kinetics and pathways of ibuprofen degradation by the UV/chlorine advanced oxidation process. *Water Res.* **2016**, *90*, 301–308. [CrossRef] [PubMed]
27. Guo, K.; Wu, Z.; Fang, J. UV-based advanced oxidation process for the treatment of pharmaceuticals and personal care products. In *Contaminants of Emerging Concern in Water and Wastewater*; Hernández-Maldonado, A.J., Blaney, L., Eds.; Elsevier Inc.: Amsterdam, The Netherlands, 2020; pp. 367–408. ISBN 9780128135617.
28. Wang, W.L.; Wu, Q.Y.; Li, Z.M.; Lu, Y.; Du, Y.; Wang, T.; Huang, N.; Hu, H.Y. Light-emitting diodes as an emerging UV source for UV/chlorine oxidation: Carbamazepine degradation and toxicity changes. *Chem. Eng. J.* **2017**, *310*, 148–156. [CrossRef]
29. Wu, Z.; Guo, K.; Fang, J.; Yang, X.; Xiao, H.; Hou, S.; Kong, X.; Shang, C.; Yang, X.; Meng, F.; et al. Factors affecting the roles of reactive species in the degradation of micropollutants by the UV/chlorine process. *Water Res.* **2017**, *126*, 351–360. [CrossRef] [PubMed]
30. Deng, J.; Wu, G.; Yuan, S.; Zhan, X.; Wang, W.; Hu, Z.H. Ciprofloxacin degradation in UV/chlorine advanced oxidation process: Influencing factors, mechanisms and degradation pathways. *J. Photochem. Photobiol. A Chem.* **2019**, *371*, 151–158. [CrossRef]
31. Guo, K.; Wu, Z.; Shang, C.; Yao, B.; Hou, S.; Yang, X.; Song, W.; Fang, J. Radical Chemistry and Structural Relationships of PPCP Degradation by UV/Chlorine Treatment in Simulated Drinking Water. *Environ. Sci. Technol.* **2017**, *51*, 10431–10439. [CrossRef]
32. Guo, Z.; Lin, Y.; Xu, B.; Huang, H.; Zhang, T.; Tian, F.; Gao, N. Degradation of chlortoluron during UV irradiation and UV/chlorine processes and formation of disinfection by-products in sequential chlorination. *Chem. Eng. J.* **2016**, *283*, 412–419. [CrossRef]
33. Dong, H.; Qiang, Z.; Hu, J.; Qu, J. Degradation of chloramphenicol by UV/chlorine treatment: Kinetics, mechanism and enhanced formation of halonitromethanes. *Water Res.* **2017**, *121*, 178–185. [CrossRef]
34. Alegre, M.L.; Geronees, M.; Rosso, J.A.; Bertolotti, S.G.; Braun, A.M.; Marrtire, D.O.; Gonzalez, M.C. Kinetic Study of the Reactions of Chlorine Atoms and $Cl_2^{\bullet-}$ Radical Anions in Aqueous Solutions. 1. Reaction with Benzene. *J. Phys. Chem. A* **2000**, *104*, 3117–3125. [CrossRef]
35. Deborde, M.; Gunten, U. Von Reactions of chlorine with inorganic and organic compounds during water treatment—Kinetics and mechanisms: A critical review. *Water Res.* **2008**, *42*, 13–51. [CrossRef]
36. Zou, H.; Tang, H. Comparison of different bacteria inactivation by a novel continuous-flow ultrasound/chlorination water treatment system in a pilot scale. *Water* **2019**, *11*, 258. [CrossRef]
37. Blume, T.; Neis, U. Improving chlorine disinfection of wastewater by ultrasound application. *Water Sci. Technol.* **2005**, *52*, 139–144. [CrossRef] [PubMed]
38. Lambert, N.; Rediers, H.; Hulsmans, A.; Joris, K.; Declerck, P.; De Laedt, Y.; Liers, S. Evaluation of ultrasound technology for the disinfection of process water and the prevention of biofilm formation in a pilot plant. *Water Sci. Technol.* **2010**, *61*, 1089–1096. [CrossRef] [PubMed]
39. Hamdaoui, O.; Merouani, S.; Ait Idir, M.; Benmahmoud, H.C.; Dehane, A.; Alghyamah, A. Ultrasound/chlorine sono-hybrid-advanced oxidation process: Impact of dissolved organic matter and mineral constituents. *Ultrason. Sonochem.* **2022**, *83*, 105918. [CrossRef] [PubMed]
40. Borzelleca, J.F.; Olson, J.W.; Reno, F.E. Lifetime toxicity/carcinogenicity study of FD & C Red No. 40 (Allura Red) in Sprague-Dawley rats. *Food Chem. Toxicol.* **1989**, *27*, 701–705. [CrossRef] [PubMed]
41. Garole, V.J.; Choudhary, B.C.; Tetgure, S.R.; Garole, D.J.; Borse, A.U. Detoxification of toxic dyes using biosynthesized iron nanoparticles by photo-Fenton processes. *Int. J. Environ. Sci. Technol.* **2018**, *15*, 1649–1656. [CrossRef]
42. Vorhees, C.V.; Butcher, R.E.; Brunner, R.L.; Wootten, V.; Sobotka, T.J. Development toxicity and psychotoxicity of FD and C red dye no. 40 (Allura red AC) in rates. *Toxicology* **1983**, *28*, 207–217. [CrossRef]
43. Sun, Q.; Yang, L.; Yang, J.; Liu, S.; Hu, X. Study on the interaction between Rhodamine dyes and Allura Red based on fluorescence spectra and its analytical application in soft Drinks. *Anal. Sci.* **2017**, *33*, 1181–1187. [CrossRef]
44. Vogt, R.; Schindler, R.N. Product channels in the photolysis of HOCl. *J. Photochem. Photobiol. A Chem.* **1992**, *66*, 133–140. [CrossRef]

45. Buxton, G.V.; Bydder, M.; Arthur Salmon, G. Reactivity of chlorine atoms in aqueous solution Part 1. The equilibrium $Cl^{MNsbd}+Cl^{-}Cl_2^{-}$. *J. Chem. Soc. Faraday Trans.* **1998**, *94*, 653–657. [CrossRef]
46. Buxton, G.V.; Greenstock, C.L.; Helman, W.P.; Ross, A.B. Critical review of rate constants for reactions of hydrated Electrons, hydrogen atoms and hydroxyl radicals ($^{\bullet}OH/O^{-}$) in aqueous solution. *J. Phys. Chem. Ref. Data* **1988**, *17*, 515–886. [CrossRef]
47. Pubchem. Allura Red AC. 2020. Available online: https://pubchem.ncbi.nlm.nih.gov/compound/Allura-Red-AC (accessed on 9 September 2022).
48. Pétrier, C.; Francony, A. Ultrasonic waste-water treatment: Incidence of ultrasonic frequency on the rate of phenol and carbon tetrachloride degradation. *Ultrason. Sonochem.* **1997**, *4*, 295–300. [CrossRef]
49. Merouani, S.; Hamdaoui, O.; Saoudi, F.; Chiha, M. Influence of experimental parameters on sonochemistry dosimetries: KI oxidation, Fricke reaction and H_2O_2 production. *J. Hazard. Mater.* **2010**, *178*, 1007–1014. [CrossRef] [PubMed]
50. Tauber, A.; Mark, G.; Schuchmann, H.-P.; von Sonntag, C. Sonolysis of tert-butyl alcohol in aqueous solution. *J. Chem. Soc. Perkin Trans. 2* **1999**, *2*, 1129–1136. [CrossRef]
51. Kong, X.; Jiang, J.; Ma, J.; Yang, Y.; Liu, W.; Liu, Y. Degradation of atrazine by UV/chlorine: Efficiency, influencing factors, and products. *Water Res.* **2016**, *90*, 15–23. [CrossRef]
52. Huang, N.; Wang, T.; Wang, W.; Wu, Q.; Li, A.; Hu, H. UV/chlorine as an advanced oxidation process for the degradation of benzalkonium chloride: Synergistic effect, transformation products and toxicity evaluation. *Water Res.* **2017**, *114*, 246–253. [CrossRef]
53. Chadi, N.E.; Merouani, S.; Hamdaoui, O.; Bouhelassa, M. New aspect of the effect of liquid temperature on sonochemical degradation of nonvolatile organic pollutants in aqueous media. *Sep. Purif. Technol.* **2018**, *200*, 68–74. [CrossRef]
54. Henglein, A. Sonolysis of carbon dioxide, nitrous oxide and methane in aqueous solution. *Z. Naturforsch. B* **1985**, *40*, 100–107. [CrossRef]
55. Harada, H.; Ono, Y. Improvement of the rate of sono-oxidation in the presence of CO_2. *Jpn. J. Appl. Phys.* **2015**, *54*, 52–55. [CrossRef]
56. Rooze, J. *Cavitation in Gas-Saturated Liquids*; Technische Universiteit Eindhoven: Eindhoven, The Netherlands, 2017. [CrossRef]
57. Merouani, S.; Hamdaoui, O.; Al-Zahrani, S.M. Toward understanding the mechanism of pure CO_2-quenching sonochemical processes. *J. Chem. Technol. Biotechnol.* **2020**, *95*, 553–566. [CrossRef]
58. Gao, Y.Q.; Gao, N.Y.; Deng, Y.; Gu, J.S.; Gu, Y.L.; Zhang, D. Factors affecting sonolytic degradation of sulfamethazine in water. *Ultrason. Sonochem.* **2013**, *20*, 1401–1407. [CrossRef] [PubMed]
59. Ferkous, H.; Hamdaoui, O.; Merouani, S. Sonochemical degradation of naphthol blue black in water: Effect of operating parameters. *Ultrason. Sonochem.* **2015**, *26*, 40–47. [CrossRef] [PubMed]
60. Boutamine, Z.; Merouani, S.; Hamdaoui, O. Sonochemical degradation of Basic Red 29 in aqueous media. *Turk. J. Chem.* **2017**, *41*, 99–115. [CrossRef]
61. Hamdaoui, O.; Merouani, S. Improvement of Sonochemical Degradation of Brilliant Blue R in Water Using Periodate Ions: Implication of Iodine Radicals in the Oxidation Process. *Ultrason. Sonochem.* **2017**, *37*, 344–350. [CrossRef] [PubMed]
62. Merouani, S.; Ferkous, H.; Hamdaoui, O.; Rezgui, Y.; Guemini, M. New interpretation of the effects of argon-saturating gas toward sonochemical reactions. *Ultrason. Sonochem.* **2015**, *23*, 37–45. [CrossRef] [PubMed]
63. Rooze, J.; Rebrov, E.V.; Schouten, J.C.; Keurentjes, J.T.F. Dissolved gas and ultrasonic cavitation—A review. *Ultrason. Sonochem.* **2013**, *20*, 1–11. [CrossRef]
64. Rooze, J.; Rebrov, E.V.; Schouten, J.C.; Keurentjes, J.T.F. Effect of resonance frequency, power input, and saturation gas type on the oxidation efficiency of an ultrasound horn. *Ultrason. Sonochem.* **2011**, *18*, 209–215. [CrossRef]
65. Chadi, N.E.; Merouani, S.; Hamdaoui, O.; Bouhelassa, M.; Ashokkumar, M. H2O2/Periodate (IO_4^{-}): A novel advanced oxidation technology for the degradation of refractory organic pollutants. *Environ. Sci. Water Res. Technol.* **2019**, *5*, 1113–1123. [CrossRef]
66. Ferkous, H.; Merouani, S.; Hamdaoui, O.; Pétrier, C. Ultrasonics Sonochemistry Persulfate-enhanced sonochemical degradation of naphthol blue black in water: Evidence of sulfate radical formation. *Ultrason. Sonochem.* **2017**, *34*, 580–587. [CrossRef]
67. Bekkouche, S.; Merouani, S.; Hamdaoui, O.; Bouhelassa, M. Efficient photocatalytic degradation of Safranin O by integrating solar-UV/TiO_2/persulfate treatment: Implication of sulfate radical in the oxidation process and effect of various water matrix components. *J. Photochem. Photobiol. A Chem.* **2017**, *345*, 80–91. [CrossRef]
68. Villaroel, E.; Silva-Agredo, J.; Petrier, C.; Taborda, G.; Torres-Palma, R.A. Ultrasonic degradation of acetaminophen in water: Effect of sonochemical parameters and water matrix. *Ultrason. Sonochem.* **2014**, *21*, 1763–1769. [CrossRef] [PubMed]
69. Merouani, S.; Hamdaoui, O.; Saoudi, F.; Chiha, M. Sonochemical degradation of Rhodamine B in aqueous phase: Effects of additives. *Chem. Eng. J.* **2010**, *158*, 550–557. [CrossRef]